ELSEVIER

Thermochimica Acta 308 (1998) 93–99

thermochimica acta

Characteristics of thermotropic phase transition of glycosphingolipid (Ganglioside) aggregates in aqueous solution[1]

Mitsuhiro Hirai*, Shigeki Arai, Toshiharu Takizawa, Sadato Yabuki, Yoshirou Nakata

Department of Physics, Gunma University, 4-2 Aramaki, Maebashi 371, Japan

Received 30 May 1997; accepted 17 June 1997

Abstract

In this report, by using synchrotron radiation X-ray small-angle scattering, we show the structural characteristics of the ganglioside aggregates depending on both the temperature and oligosaccharide chain. The experimental results of the aqueous solutions containing G_{M1}, G_{D1}, or crude mixture gangliosides show that the elevation of temperature induces the change of the micellar structure accompanied by the change of the internal scattering density distribution. These changes are well described by applying a shell-modeling method to the observed scattering curves since the shell-modeling method can determine the intramicellar structures. A noticeable common feature found in the thermotropic transition of the ganglioside micelles is the contraction of the micellar dimension resulting from the shrinkage of the hydrophilic region of the micelle. The shrinkage amounts to 20–30% of the thickness of the hydrophilic region, suggesting the structural change of the oligosaccharide chains of the gangliosides from an extended conformation to a compact one. The differences of the thermotropic stability depending on the number of the sialic acids of the oligosaccharide chain were also observed. The present results which suggest a thermal perturbation in the physiological range 20–50°C induces a conformational change of the oligosaccharide chains of ganglioside molecules very sensitively. © 1998 Elsevier Science B.V.

Keywords: Ganglioside; Glycolipid; Hydration; Micelle; Sialoglycosphingolipid; Small-angle scattering; Synchrotron radiation; Thermotropic phase transition

Keywords: G_{M1}, (II^3NeuAc-GgOse$_4$-Cer); G_{D1a}, (IV^3NeuAc-, II^3NeuAc-GgOse$_4$-Cer); G_{D1b}, (II^3NeuAc$_2$-GgOse$_4$-Cer)

1. Introduction

Gangliosides have been studied intensively on the physiological role relating to a variety of surface events such as molecular recognition of external ligands, self organization of tissues, immune response and cell differentiation [1–3]. Gangliosides, the most abundant complex of the glycosphingolipids in the plasma membrane of nerve cells with 5–10% of the total lipid mass, are characterized by the presence of an oligosaccharide chain, containing one or more *N*-acetylneuraminic acid (called sialic acid) residues. A very amphiphilic property of ganglioside compared to other membrane lipids is attributable to an oligosaccharide chain which links to a ceramide.

*Corresponding author. Tel.: 0081 27220 7552; fax: 0081 27220 7554; e-mail: hirai@sun.aramaki.gunma-u.ac.jp

[1]Presented at the 14th IUPAC Conference on Chemical Thermodynamics, held in Osaka, Japan, 15–30 August, 1996.

PII S0040-6031(97)00335-3

The presence of oligosaccharide chains as hydrophilic moieties lead gangliosides to form aggregates or mixed aggregates with other amphiphilic molecules in aqueous solution. In spite of the physicochemical and structural studies of ganglioside aggregates and mixtures with other lipids by many investigators [4–8], there have been less direct evidence showing structural properties of ganglioside aggregates. In connection with a phase behavior we have been studying structural properties and functions of micellar (including reversed micellar) or lamellar systems composed of other amphiphilic phospholipid [9–13] or surfactant/protein/organic solvent [14,15] by using scattering techniques, calorimetry and NMR spectroscopy. Recently, by using neutron and X-ray scattering techniques we have reported on the complexation process of ganglioside aggregates with proteins [16], the internal structures and thermotropic structural changes of ganglioside micelles (G_{M1} and G_{D1}) in aqueous solution [17–19]. In this paper, we will compare the thermotropic properties of different types of ganglioside aggregates (G_{M1}, G_{D1} and a crude mixture) in aqueous solution and clarify their common feature in a thermotropic phase behavior.

2. Experimental

2.1. Samples and small-angle X-ray scattering measurements

Three different types of gangliosides extracted from bovine brain were used. The gangliosides were monosialoganglioside G_{M1} (II^3NeuAc-GgOse$_4$-Cer), disialoganglioside G_{D1} (IV^3NeuAc-, II^3NeuAc-GgOse$_4$-Cer (G_{D1a})+ II^3NeuAc$_2$-GgOse$_4$-Cer (G_{D1b})) and type-II ganglioside (containing 15% sialic acid). G_{M1} and type-II were purchased from Sigma. G_{D1} was prepared in our laboratory as described elsewhere [20]. By using thin-layer chromatography we confirmed that the ganglioside molecular species in the type-II are composed of more than three ganglioside components, as reported [21]. The type-II ganglioside sample was regarded as a crude mixture. As shown by HPLC procedure [22], the lipidic portion (namely, the ceramide) of the natural ganglioside extracted from bovine brain is primarily composed of a long-chain fatty acid (stearic acid which covers 90% or more of the total fatty acid content) and a long-chain base (C_{18} and C_{20} unsaturated sphingosine which is generally more than 10% of the total content). The ganglioside solutions of 0.5% w/v in buffer adjusted to pH 6.8 were prepared and used for the scattering measurements.

Small-angle X-ray scattering experiments were performed by using the synchrotron radiation small-angle X-ray scattering spectrometer installed at BL10C line of the 2.5 GeV storage ring at the Photon Factory at the National Laboratory for High Energy Physics, Tsukuba, Japan [23]. The wavelength used was 1.49 Å and each exposure time for one measurement was 100 s. The ganglioside solution was contained in a sample cell which was placed in a cell holder controlled from 6 to 60°C.

2.2. Scattering data analysis and modeling methods

The scattering curves $I(q)$ were analyzed as follows. The distance distribution function $p(r)$, which reflects the particle shape and the intraparticle scattering density distribution [24], is obtained by the Fourier transform of the scattering intensity $I(q)$ as

$$p(r) = \frac{2}{\pi}\int_0^\infty rqI(q)\sin(rq)\mathrm{d}q \tag{1}$$

where q is the magnitude of scattering vector defined by $q=(4\pi/\lambda)\sin(\theta/2)$ (θ, the scattering angle; λ, the wavelength). The maximum dimension D_{max} of the particle can be estimated from the $p(r)$ function satisfying the condition $p(r)=0$ for $r>D_{max}$. To avoid some systematic error which often occurs on the estimation of the radius of gyration R_g by the use of the Guinier approximation ($\ln(I(q))$ vs. q^2 plot), we used the Glatter's method where the R_g is given by [24]

$$R_g^2 = \frac{\int_0^{D_{max}} p(r)r^2\mathrm{d}r}{2\int_0^{D_{max}} p(r)\mathrm{d}r} \tag{2}$$

As we have shown elsewhere [12–15,17–19], the shell-modeling method takes an advantage to fit the experimental data for determination of micellar structural parameters. The spherically averaged scattering function $I(q)$ from a particle described by n shells

different average scattering densities is simply given by

$$I(q) = \int_0^1 \left[3\left\{\bar{\rho}_1 V_1 j_1(qR_1)/(qR_1) + \sum_{i=2}^{n}(\bar{\rho}_i - \bar{\rho}_{i-1})V_i j_1(qR_i)/(qR_i)\right\}\right]^2 \mathrm{d}x \quad (3)$$

where $\bar{\rho}_i$ and V_i are the average excess scattering density (called contrast) and the volume of ith shell with an ellipsoidal shape of rotation, j_1 is the spherical Bessel function of the first rank. R_i is defined as

$$R_i = r_i(1 + x^2)(v_i^2 - 1))^{1/2} \quad (4)$$

where r_i and v_i are the semi-axis and the semi-axis ratio of ith ellipsoidal shell, respectively. $\bar{\rho}_i$, r_i and v_i were used as fitting parameters.

3. Results and discussion

3.1. Variation of scattering curve and distance distribution function depending on temperature

Fig. 1 shows the temperature dependence of the scattering curves of the different ganglioside solutions, where Fig. 1(a), (b) and (c) correspond to G_{M1}, G_{D1} and type-II gangliosides, respectively. Every scattering curve is characterized by the minimum at $q \approx 0.065$–0.05 Å^{-1} and the rounded peak at $q \approx 0.09$–0.1 Å^{-1}, which reflect the presence of particles with an identical globular shape. The difference in the scattering profiles of (a), (b) and (c) is ascribed to the solute particle structure, which is shown in the following modeling analyses. The saturating tendencies in the scattering curve below $q \approx 0.04$ Å^{-1} with the evident minimum at $q \approx 0.065$–0.05 Å^{-1} indicate monodispersities of the present aqueous solution systems. If there had been some polydispersity of the solute particles in shape or dimension, the scattering curve would have been rather smeared. For all ganglioside samples the changes of the scattering curves occur with shifting the position of the rounded peak to a slightly higher q value, indicating the structural transitions of the micelles caused by the elevation

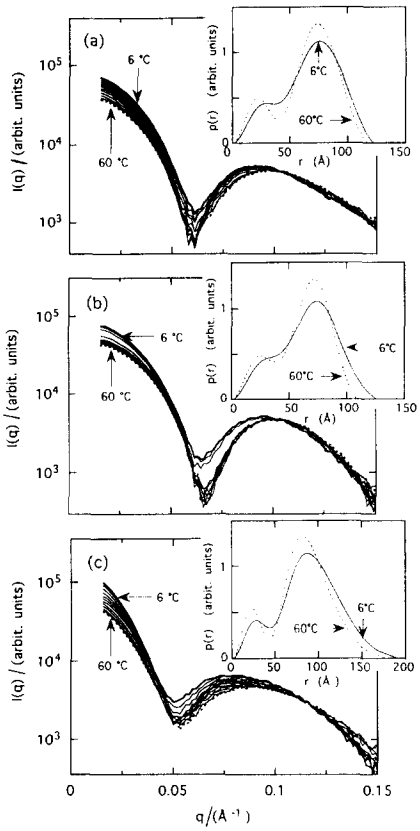

Fig. 1. Thermotropic changes of the scattering curves $I(q)$ and distance distribution functions $p(r)$ of ganglioside micelles in aqueous solution. (a) G_{M1}, (b) G_{D1}, (c) type-II (crude mixture). The inserts in (a), (b) and (c) show the $p(r)$ functions of 6 and 60°C.

of temperature. The temperature range where the change of the scattering curve occurs more remarkably depends on the samples, namely, the range of 40–50°C for G_{M1}, 15–25°C for G_{D1} and 6–20°C for type-II. The change of the scattering curve for G_{M1} occurs more continuously compared with that of G_{D1}.

The inserts in Fig. 1 show the distance distribution functions $p(r)$ corresponding to the scattering curves of 6 and 60°C. Every $p(r)$ profile is characterized by the shoulder (or hump) around 30 Å and the bell-shaped peak locating at ca. 75–80 Å, which is a typical feature of the internal scattering density distribution of the solute particle which is composed of a core with negative excess average scattering density (negative contrast) surrounded by a shell with positive contrast [25]. The ganglioside molecule consists of a ceramide (hydrocarbon tail) and an oligosaccharide chain with

sialic acids (hydrophilic head), whose moieties have negative and positive contrasts, respectively. Thus, the $p(r)$ profiles obtained above well reflect the characteristics of the micellar structures of the ganglioside aggregates [17–19]. The elevation of the temperature induces the increase of the peak height and the change of the shoulder shape around 30 Å with the shifts of the peak and intercept (satisfying $p(r)=0$ for $r>0$) positions to smaller r values. The $p(r)$ function depends on both the particle geometry and the intraparticle scattering density distribution. Then, such changes of the $p(r)$ profiles are attributable both to the change of the intramicellar structure and the contraction of the maximum dimension of the micelle, which are common features induced by the temperature elevation for G_{M1}, G_{D1} and type-II gangliosides. The above changes of the $p(r)$ profiles can be explained by the shrinkage of the hydrophilic region, as shown in the following modeling analyses.

3.2. *Modeling analyses and temperature dependence of structural parameters*

The gyration radii R_g obtained from the experimental data by using Eq. (2) are shown in Fig. 2. In a solution system composed of same particles, the gyration radius R_g of the particle is given by

$$R_g^2 = \int_V r^2 dr/V + \int_V \rho_f(r) r^2 dr/(\bar{\rho}V) \qquad (5)$$

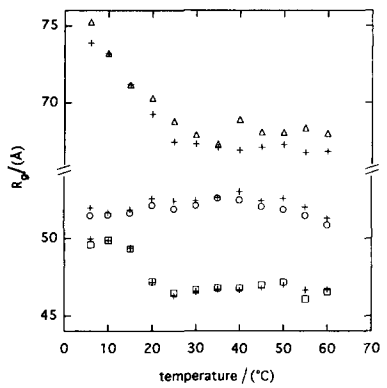

Fig. 2. Temperature dependence of the gyration radii determined by the Glatter method. The experimental values are shown by the open marks; ○ G_{M1}, □ G_{D1}, Δ type-II. + marks represent the gyration radii obtained from the shell-modeling analysis.

where $\bar{\rho}$, $\rho_f(r)$ and V are the average contrast, the intraparticle scattering density fluctuation around $\bar{\rho}$, and the particle volume, respectively. For a particle with a homogeneous internal scattering density distribution such as a hard particle the second term in Eq. (5) is null, then the change of the R_g simply reflects the change of the shape or dimension of the particle. For a particle with an arbitrary internal scattering density fluctuation ($\rho_f(r) \neq 0$) such as ganglioside micelles, the change of the $\rho_f(r)$ also affects the R_g value by the second term in Eq. (5). In Fig. 2, the R_g of the G_{M1} micelle once increases from 51.5 to 52.6 Å in the range of 6–35°C and decreases to 50.9 Å. The R_g of the G_{D1} significantly decreases from 49.8 to 46.5 Å in the range of 15–25°C, and mostly retains above 25°C. The R_g of the type-II ganglioside significantly decreases from 75.2 to 68.0 Å in the range of 6–25°C. In both cases of the G_{D1} and type-II ganglioside micelles the variation of the R_g value caused by elevating temperature is remarkable in the range of 6–25°C, while in the case of the G_{M1} the variation of the R_g is relatively small in spite of the systematic change of the scattering profile in Fig. 1(a). As presented by the cross marks in Fig. 2, the changing process of the R_g for the different ganglioside samples can be well explained by the following shell-modeling analyses using Eq. (3).

To discuss the above thermotropic transition in detail, we used the shell-modeling analysis on the assumption of monodispersity. As shown in our previous reports [17–19], the shell-modeling method is very useful to describe the experimental data for the determination of the structural parameters of the system composed of particles with a same center-symmetrical internal scattering density distribution. The ganglioside micelle can be described well as an ellipsoid consisting of a core and a shell since the scattering density of the hydrophilic head (the oligosaccharide chain with sialic acids) greatly differs from that of the hydrophobic tail (the ceramide with two hydrocarbon chains). Fitting parameters were the radii of the shell and core, the axial ratios and the average contrasts. Fig. 3 and the inserts show the simulated scattering curves and distance distribution functions corresponding to 6 and 60°C, which describe well the experimental ones. The reliability factors R for the present optimized models, defined as $R = \sum_{q=q_{min}}^{q_{max}} |I_{obs}(q) - I_{model}(q)| / \sum_{q=q_{min}}^{q_{max}} I_{obs}(q)$ (where

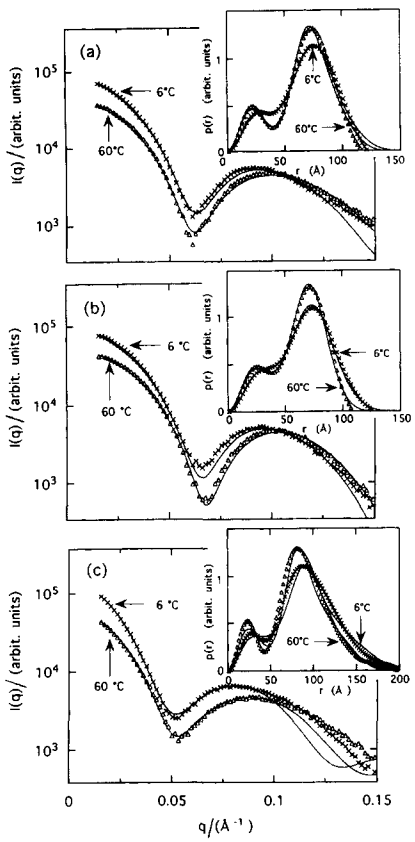

Fig. 3. Scattering curves $I(q)$ and distance distribution functions $p(r)$ obtained from the shell-modeling analysis. (a), (b) and (c) as in Fig. 1. The inserts show the $p(r)$ functions. X and Δ marks represent the experimental $I(q)$ and $p(r)$ of 6 and 60°C. Full lines are the simulated $I(q)$ and $p(r)$.

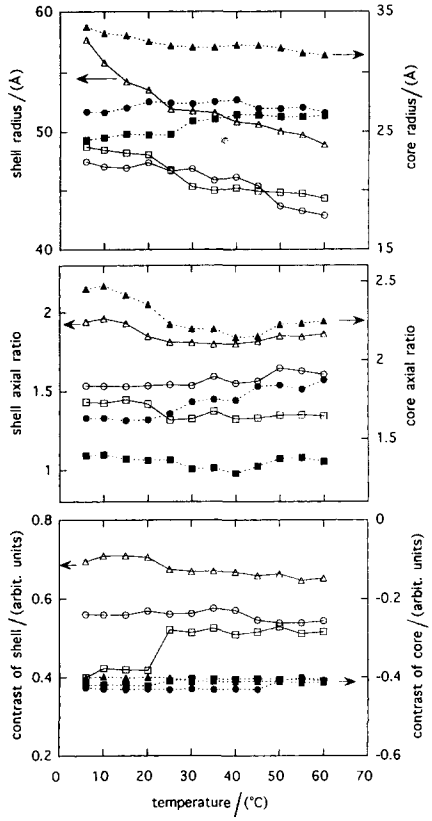

Fig. 4. Temperature dependence of the structural parameters of the ganglioside micelles determined by the shell-modeling analysis. The upper figure shows the shell and core radii, the middle figure the shell and core semiaxial ratios, and the lower figure the average excess scattering densities (called contrasts) of the shell and core, plotted as a function of temperature. ○ and ● show G_{M1}, □ and ■ G_{D1}, Δ and ▲ type-II. Open and full marks correspond to the structural parameters of the shell and the core, respectively.

q_{min} and q_{max} are the minimum and maximum values of q observed in the present scattering experiments, respectively), are in the range of 0.02–0.03 for G_{M1}, 0.02–0.04 G_{D1} and 0.04–0.07 for type-II. In the case of type-II the R factor is a little large compared with the cases of G_{M1} and G_{D1}. This suggests that the monodispersity of the type-II solution would be slightly lower than those of the G_{M1} and G_{D1} solutions. As we showed in the previous reports, the models such as a hard sphere or a hard ellipsoid without considering internal structure cannot describe the experimental scattering curves and distance distribution functions. The R_g values of the optimized models represented by+marks in Fig. 2 are also in good agreements with those obtained from the experimental data.

Fig. 4 summarizes the temperature dependence of the structural parameters of the ganglioside micelles determined by the shell-modeling analysis. In the case of G_{M1}, the shell radius gradually decreases from 47.5 to 42.9 Å in the range of 6–40°C and faster above 40°C, whereas the core radius varies slightly from 26.7 to 26.6 Å. The shell thickness, namely, the hydrophilic region, decreases from 20.8 to 16.3 Å, whose decrement is about 4.5 Å. The axial ratios of the core and the shell slightly increases above ca. 30°C from 1.63 to 1.87 and from 1.53 to 1.61, respectively. The contrasts of the core and shell mostly holds in the range from −0.43 to −0.41 and from 0.55 to 0.57, respectively. In

the case of G_{D1}, in the range of 20–30°C the shell radius evidently decreases from 48.0 to 45.3 Å and the core radius increases from 24.8 to 26.1 Å. The shell thickness decreases from 23.3 to 19.3 Å and the decrement is about 4 Å. The shell contrast shows the increase from 0.43 to 0.51, while the core contrast holds from −0.42 to −0.40. The axial ratios of the core and the shell slightly decrease from 1.38 to 1.33 and from 1.43 to 1.34, respectively. In the case of type-II, the shell radius remarkably decreases from 57.7 to 48.9 Å and the core radius slightly decreases from 33.7 to 31.4 Å. The shell thickness decreases from 23.9 to 17.5 Å and the decrement is about 6.4 Å. The axial ratios of the core and the shell show the decreasing tendencies from 2.46 to 2.23 and from 1.94 to 1.86, respectively, which is most evident in the range of 10–25°C. The shell contrast slightly decreases from 0.71 to 0.66 around 25°C, while the core scattering density mostly holds in the range from ca. −0.41 to −0.40 in the whole temperature range. It should be worthy of noticing that for a particle with a large internal scattering density heterogeneity a change of gyration radius is less sensitive to discuss a structural change, namely, that for such a particle as a ganglioside micelle the change of the internal structure greatly affects the gyration radius. In the present case, when Fig. 4 is compared with Fig. 2 the change of R_g of the G_{M1} micelle is relatively smaller than that of the G_{D1} micelle since the change of the intramicellar structure compensates for the change of R_g. Thus, to confirm a structural change of particle in detail it is important to measure scattering curves in a wide q range for applying a modeling analysis.

Common features in the thermotropic structural transitions of the ganglioside micellar solutions containing G_{M1}, G_{D1} or type-II are that the elevation of temperature induces the shrinkage of the hydrophilic region of the micelle in about 4 Å and that the contraction of the micellar dimension results from the shrinkage of this region. Comparing the thermotropic structural change of the G_{M1} micelle with that of the G_{D1} micelle, the decrement of the thickness of the hydrophilic region of the G_{M1} micelle is slightly larger than that of the G_{D1} micelle. The thickness of the hydrophilic region decreases most significantly around ca. 20–30°C for G_{D1} and ca. 40–50°C for G_{M1}. In addition the change of the G_{D1} micelle accompanies the evident decrease of the gyration radius, the increase of the contrast of the hydrophilic region and the slight expansion of the hydrophobic region. Such characteristics would reflect the differences between the thermotropic stability of the oligosaccharide chains depending on the number of the sialic acids. The type-II gangliosides, a mixture of various types of gangliosides, form much elongated ellipsoidal micelles and show much remarkable changes in both the gyration radius and the thickness of the hydrophilic region.

In general, micellar hydrocarbon cores are considered to contain many gauche bonds in the hydrocarbon chain configurations [26–28]. As shown in the previous studies [29–31], ganglioside solutions show rather broad thermotropic phase transitions which greatly depend on oligosaccharide chain characteristics. Such transitions differ evidently from those of phospholipid lamellar systems where the thermotropic phase transitions are understood as the so-called hydrocarbon chain melting. The studies using fluorescent probe method or calorimetry for ganglioside solutions indicate the changes of the packing of hydrocarbon chains depend on the head groups [29,32]. The NMR study combined with molecular dynamics calculations suggest that the geometrical property of the ganglioside aggregates depend on the intrinsic dynamic structural properties of the oligosaccharide chain [33]. To take account of those previous results, the thermotropic structural transitions of the ganglioside micelles observed would be attributable mainly to a conformational change of oligosaccharide chains from extended structures to compact ones, and in the hydrophobic portion some minor rearrangements of the hydrocarbon chains would also occur.

By the way, the oligosaccharide chains of the ganglioside micelle can be assumed to be very accessible by water and to be highly hydrated to take expanded conformations as occasionally observed in solvated polymer chains. Therefore the significant decrease of the hydrophilic region would accompany an extrusion of some amount of water from this region, which might be suggested by the increase of the contrast of the hydrophilic region in the case of the G_{D1}. Micellar hydrocarbon cores are considered to be virtually devoid of internal water. However, such an extrusion of water would also occur in the interfacial region between the hydrophilic and hydrophobic por-

tions of the ganglioside micelle since the presence of large hydrophilic heads would allow some water to penetrate to the interface. The present results suggest that the ganglioside molecules, locating generally in the outer-cell plasma membrane, can greatly modulate cell surface structures by changing the oligosaccharide chain conformations under a thermotropic perturbation. Such an intrinsic aggregation property of gangliosides would result from a high conformational flexibility of the oligosaccharide chains, which might contribute to the promotion of various physiological surface events in biomembranes.

Acknowledgements

We thank Dr. Y. Amemiya and Dr. K. Kobayashi of the Photon Factory at the National Laboratory for High Energy Physics for their help with the small-angle scattering instrumentation. This work was performed under the approval of the Photon Factory Programme Advisory Committee (Proposal No. 92-069, 93G047 & 95G084).

References

[1] S. Hakomori, Sci. Am. 254 (1986) 32.
[2] Y.A. Hannun, R.M. Bell, Science 243 (1989) 500.
[3] L. Svennerholm, A.K. Asbury, R.A. Reisfeld, K. Sandhoff, K. Suzuki, G. Tettamanti, G. Toffano (Eds.), Biological Function of Gangliosides, Elsevier, Amsterdam, 1994.
[4] S. Sonnion, L. Cantù, M. Corti, D. Acquotti, B. Venerando, Chem. Phys. Lipids 71 (1994) 21.
[5] B. Maggio, T. Ariga, J.M. Sturtevant, R.K. Yu, Biochim. Biophys. Acta 818 (1985) 1.
[6] H. Kojima, K.M. Yoshikawa, A. Katagiri, Y. Tamai, J. Biochem. 103 (1988) 126.
[7] M. Ollmann, H.J. Galla, Biochim. Biophys. Acta 941 (1988) 1.
[8] Y.-S. Tsao, F. Freire, L. Huang, Biochim. Biophys. Acta 900 (1987) 79.
[9] T. Takizawa, K. Hayashi, H. Mitomo, Thermochim. Acta 123 (1988) 247.
[10] T. Takizawa, H. Mitomo, K. Hayashi, Thermochim. Acta 163 (1990) 133.
[11] T. Takizawa, K. Hayashi, H. Mitomo, Thermochim. Acta 183 (1991) 313.
[12] M. Hirai, T. Takizawa, S. Yabuki, Y. Nakata, T. Hirai, K. Hayashi, J. Phys. Chem. 99 (1995) 17456.
[13] M. Hirai, T. Takizawa, S. Yabuki, Y. Nakata, T. Hirai, K. Hayashi, J. Chem. Soc, Faraday Trans. 92 (1996) 1493.
[14] M. Hirai, T. Takizawa, S. Yabuki, R. Kawai-Hirai, K. Nakamura, K. Kobayashi, Y. Amemiya, M. Oya, J. Chem. Soc. Faraday Trans. 91 (1995) 1081.
[15] M. Hirai, R. Kawai-Hirai, T. Takizawa, S. Yabuki, T. Hirai, K. Kobayashi, Y. Amemiya, M. Oya, J. Phys. Chem. 99 (1995) 6652.
[16] M. Hirai, S. Yabuki, T. Takizawa, Y. Nakata, H. Mitomo, T. Hirai, S. Shimizu, K. Kobayashi, M. Furusaka, K. Hayashi, Physica B, 213&214 (1995) 748.
[17] M. Hirai, T. Takizawa, S. Yabuki, Y. Nakata, H. Mitomo, T. Hirai, S. Shimizu, K. Kobayashi, M. Furusaka, K. Hayashi, Physica B, 213&214 (1995) 751.
[18] M. Hirai, T. Takizawa, S. Yabuki, Y. Nakata, K. Hayashi, Biophys. J. 70 (1996) 1761.
[19] M. Hirai, T. Takizawa, S. Yabuki, T. Hirai, K. Hayashi, J. Phys. Chem. 100 (1996) 11675.
[20] K. Hayashi, A. Katagiri, Biochim. Biophys. Acta 337 (1974) 107.
[21] E.G. Trams, C.J. Lauter, Biochim. Biophys. Acta 60 (1962) 350.
[22] S. Sonnino, D. Acquotti, L. Riboni, A. Giuliani, G. Kirschner, G. Tettamanti, Chem. Phys. Lipids 42 (1986) 3.
[23] T. Ueki, Y. Hiragi, M. Kataoka, Y. Inoko, Y. Amemiya, Y. Izumi, H. Tagawa, Y. Muroga, Biophys. Chem. 23 (1985) 115.
[24] O. Glatter, In Small Angle X-ray Scattering, in: O. Glatter, O. Kratky (Eds.), Academic Press, London, 1982, p. 119.
[25] M. Hirai, T. Hirai, T. Ueki, Macromolecules 27 (1994) 1003.
[26] D.W.R. Gruen, J. Colloid Interface Sci. 84 (1981) 281.
[27] D.W.R. Gruen, E.H.B. de Lacey, Surfactants in Solution, in: K.L. Mittel, B. Lindman (Eds.), Vol. 1, Plenum Press, New York, 1984, p. 279.
[28] K.A. Dill, D.E. Koppel, R.S. Cantor, J.D. Dill, D. Bendedouch, S.-H. Chen, Nature 309 (1984) 42.
[29] D. Bach, I.R. Miller, B.-A. Sela, Biochim. Biophys. Acta 686 (1982) 233.
[30] B. Maggio, T. Ariga, J.M. Sturtvant, R.K. Yu, Biochemistry 24 (1985) 1084.
[31] T. Takizawa, K. Hayashi, Abstracts Papers of The International and the Third Sino-Japanese Joint Symposium on Thermal Measurements, Xi'an, China, June 6–9, 1994, p. 46.
[32] T. Uchida, Y. Nagai, Y. Kawasaki, N. Wakayama, Biochemistry 20 (1981) 162.
[33] D. Acquotti, L. Cantu, E. Ragg, S. Sonnino, Eur. J. Biochem. 225 (1994) 271.